

Searching for Imprints of Circumstellar Material in the Ultraviolet Spectra of Type Ia Supernovae

Aaron Beaudoin^{1,2*}, Ryan J. Foley^{1,2}

¹*Astronomy Department, University of Illinois at Urbana–Champaign, 1002 W. Green Street, Urbana, IL 61801, USA*

²*Department of Physics, University of Illinois Urbana–Champaign, 1110 W. Green Street, Urbana, IL 61801, USA*

Accepted . Received ; in original form

ABSTRACT

This is my abstract.

Key words: supernovae: general – supernovae: individual: SN 2014J

1 INTRODUCTION

Type Ia supernovae (SNe Ia) have relatively homogeneous luminosities, making them excellent probes of dark energy and the accelerating expansion of the universe. There are multiple theories regarding their progenitor systems, the two most widely accepted being the single-degenerate (SD) and the double-degenerate (DD) models. The former consists of a white dwarf accreting material from either a main-sequence or red-giant star until it reaches the Chandrasekhar mass limit, igniting a thermonuclear explosion. The latter consists of two white dwarfs, where one accretes material onto the other or they collide, where either will also ignite a thermonuclear explosion. However, there is still much uncertainty regarding these systems, and developing a greater understanding of the circumstellar material surrounding SNe Ia is essential in fully understanding these explosions and using them to put greater constraints on dark energy.

The Na doublet located around 5890 and 5896 angstroms has been measured and analyzed in multiple studies and has shown variability in a handful of cases. This suggests that the Na gas is within 0.5 pc (because of an ionization potential of 5.1 eV) surrounding the SN is ionized by the initial flash. Later, as the Na recombines, absorption features will begin to appear in the SNs spectrum. However, we need more information from other species with similar ionization potentials to Na in order to determine the circumstellar gas location, density, and distribution.

This work presents the first insight into the Mg II, Mg I, and Fe II absorption features found in the ultraviolet spectrum of 8 SNe Ia, and is the first attempt to probe gas other than Na I, Ca II (not useful because it has a high ionization potential), and KI (not useful because its features are remarkably weak; although a recent result by (Graham et al. 2015) does detect the weakening of the two most blueshifted components with velocities of 144 and 127 km s^{-1}). These features have rest wavelengths of 2796.35 Å and 2803.53

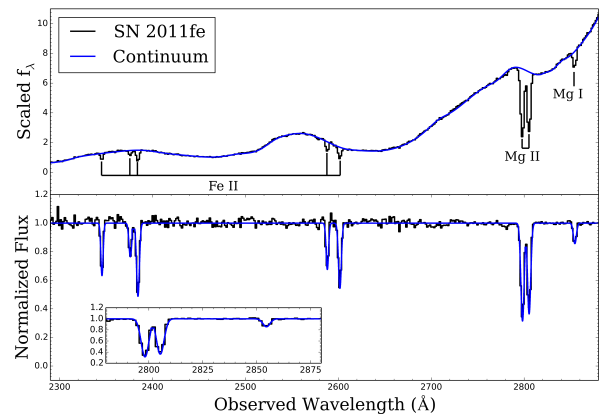


Figure 1. (Top) Maximum-brightness spectrum of SN 2011fe. The blue curve is a 3rd-order interpolated fit to the data including Gaussian profiles for the Fe II $\lambda\lambda$ 2344, 2374, 2383, 2587, 2600; Mg II $\lambda\lambda$ 2796, 2803; and Mg I λ 2853 absorption features. (Bottom) Normalized maximum-brightness spectrum of SN 2011fe. The inset is a zoom-in showing the region near the Mg I and Mg II features.

Å for the Mg II doublet, 2852.96 Å for the Mg I line, and 2344.21 Å, 2374.46 Å, 2382.76 Å, 2586.65 Å, and 2600.17 Å for the Fe II lines (Aldenius et al. 2006), and can be seen in in the top panel of Figure 1. With ionization potentials 7.6 eV and 7.9 eV for Mg and Fe, respectively, these ions have the potential to add additional constraints on the location of circumstellar material surrounding SNe Ia.

2 OBSERVATIONS AND DATA REDUCTION

Our sample consists of all SNe Ia with at least two relatively high resolution ($R > 500$) and high signal-to-noise ratio (S/N) spectra that cover at least the Mg II doublet. This limits the sample to 8 SNe Ia, all observed by the *Hubble Space Telescope* (HST). With the exception of one SN,

* E-mail: beaudoi1@illinois.edu

all spectra were obtained with the Space Telescope Imaging Spectrograph (STIS). SN 1992A was observed with the Faint Object Spectrograph (FOS). Spectra for SNe 1992A, 2011by, 2011fe, 2011iv, and 2014J were first published elsewhere (Kirshner et al. 1993; Foley et al. 2012, 2014; Foley 2013; Foley & Kirshner 2013a; ?, ?). All spectra were reduced in a consistent manner following standard procedures (e.g., Foley et al. 2012).

Half the sample have only two or three epochs of spectroscopy, while the other half have ≥ 7 epochs. Details of the SNe are presented in Table 2. A log of all observations are listed in Table 3.

In all spectra, we see clear narrow absorption features from the Mg II doublet. However, for three SNe, only lines consistent with Milky Way absorption are detected (SNe 1992A, 2011iv, and 2011ek). This is not unexpected for these objects since SNe 1992A and 2011iv have early-type hosts and SN 2011ek occurs at a projected distance of >10 kpc from its host. For the other 5 SNe Ia, we detect measurable Mg II in at least one spectrum. For all SNe with detectable Mg II, we have also detected Mg I $\lambda 2851$, and only SN 2011by, 2011fe, and 2013dy have detectable Fe II absorption.

3 ANALYSIS

With detections of several absorption features, we now detail how we make our equivalent width (EW) measurements, determine limits for undetected lines, and verify our measurements.

In order to measure the EWs of the narrow absorption features, we first fit a 3rd order b-spline to the continuum. The knots used in the interpolation are set with manually inputted breakpoints throughout the continuum between $2000 - 3000 \text{ \AA}$. Because this region is the only part of the spectrum that these lines are present, we place equally spaced breakpoints (one for every 10, 12, or 17 pixels, based on S/N) elsewhere in the continuum. We then generate a normalized spectrum by dividing this fit from the continuum. Because the spectral resolution is low enough where the absorption features are unresolved, we fit Gaussian parameters (height, width, and redshift) to the absorption features using a least-squares minimization. A normalized spectrum and its Gaussian fit can be seen in the bottom panel of Figure 1. Because of the low S/N of some spectra this method is preferable to a direct measurement, which can be significantly biased by the exact wavelength range chosen for integration. Then, we integrate over this Gaussian function to measure the equivalent width of each absorption feature, and use Equation 1 to determine the statistical error. σ_h and σ_w are found by taking the square root of the product of the reduced covariance and the reduced chi squared for the height and width, respectively, where the reduced covariance matrix is returned by the least squares algorithm.

$$\sigma_{\text{tot}}^2 = \sqrt{\pi} \times (\sigma_h^2 \times w^2 + \sigma_w^2 \times h^2) \quad (1)$$

For SNe 2011by, 2012cg, and 2013dy, the Milky Way Mg II $\lambda 2803$ line overlaps in wavelength with the host-galaxy Mg II $\lambda 2796$ line. For 11fe and 14J, both lines overlap. For these objects, we fit the entire feature (both Mg II doublets) with two Mg II doublets, one at zero velocity and the other

at roughly the recession velocity of the host galaxy, simultaneously. Because of degeneracies in the fitting, we fixed each line from a given doublet to have the same shape. As a result for these objects, the EW for one Mg II line is equivalent to that of the other. However, the additional data from the overlapping line is useful for constraining parameters and improves the accuracy of the EW measurement. To make these measurements, we use the same least-squares minimization algorithm to fit for the Gaussian parameters of all four absorption features simultaneously.

In addition to the statistical uncertainties determined during the Gaussian fitting, we estimated the systematic uncertainties, mostly resulting from uncertain continuum placement, through a Monte Carlo simulation. For each realization of the Monte Carlo simulation, we shift the nominal wavelength of the b-spline breakpoints and recreate the normalized continuum. The amplitudes of the shifts are chosen such that the continuum is not obviously incorrect for 95% of 500 sample trials. We then measure the EWs of each line with the new normalized spectrum. The scatter in the resulting distribution of EW measurements was used to determine the systematic uncertainty. The statistical and systematic uncertainties were combined for our total uncertainty.

In some spectra, we do not detect any resolvable absorption. In such cases, we determined the magnitude necessary for each Fe and Mg absorption feature to be detected within the noise of a specific normalized spectrum. In SN 1992A, 2011ek, and 2011iv, we only detect absorption consistent with Milky Way measurements, and we cannot detect certain features in some other spectra from the other SNe, which are represented in Table 4 as values without uncertainty values. To find these values, we determined the 3σ limit with Equation 2 (Leonard & Filippenko 2001).

$$W_\lambda(3\sigma) = 3\Delta\lambda\Delta I \sqrt{\frac{W_{\text{line}}}{\Delta\lambda}} \sqrt{\frac{1}{B}}, \quad (2)$$

, where ΔI is the RMS fluctuations of the normalized flux and B is the number of bins per resolution element (2). Because the width of the line is at the resolution of the spectrum, $\Delta\lambda$ (the spectral resolution is 2 or 3 pixels) and W_{line} (the estimated width of the feature) are the same.

Finally, we determine if any variability in these features would be detected within the resolution of our data by convolving the Na absorption features from SN 2006X to the resolution of our data ($.008 \text{ \AA}$ per pixel to 1.5 \AA per pixel). This process involves scaling the redder Na (5889.95 \AA) line to the wavelength of both of the Mg II features and placing it into a normalized spectrum, creating a synthesized Mg II doublet. We then shift this to a velocity scale and perform a convolution on the data using an AstroPy function that uses a Gaussian kernel with a size of 1.5 \AA . We then take the convolved data and rebin it to the pixel size of the data for our SNe (1.38 or 1.5 \AA per pixel). Using the same process as making our prior measurements, we look for variability over time. Because the Na in SN 2006X data has already been confirmed to change by (?), we were able to determine that we will detect any possible variability in our data.

Using these convolved spectra, we add in random noise based on the RMS of the spectra

Table 1. Equivalent Width vs. Dust Reddening

SN	MgII (2796.35 Å)	MgII (2803.53 Å)	$A_{V(MW)}$ (mag)	$E(B-V)_{host}$ (mag)
<i>SN1992A</i>			0.047	0.00
<i>SN2011by</i>			0.038	0.012
<i>SN2011ek</i>			0.979	0.18
<i>SN2011fe</i>			0.024	0.008
<i>SN2011iv</i>			0.031	0.011
<i>SN2012cg</i>			0.057	0.18
<i>SN2013dy</i>			0.421	$0.206 \pm .005$
<i>SN2014J</i>			0.435	1.2

4 RESULTS

These are my results, seen in Figure ??.

In our best measurements to date, we do not detect any significant change in any of the absorption features, consistent with studies of optical features for SN 2011fe (Patat et al., 2013) and SN 2014J (Welty et al., 2014; Goobar et al., 2014, Foley et al., 2014). We therefore do not detect a large amount of CSM along our line of sight.

5 DISCUSSION

We also show the equivalent width values we measured for each SNe with the corresponding reddening data for both the Milky Way and the host galaxy in Table 1. Each A_V value was taken from the NASA/IPAC Extragalactic Database and the $E(B_V)$ values were found in (Kirshner et al. 1993), (Foley & Kirshner 2013b), (Silverman et al. 2012), (Foley & Kirshner 2013b), (Foley et al. 2012), (Silverman et al. 2012), (Pan et al. 2015), and (Goobar et al. 2014) for SN 1992A, SN 2011by, SN 2011ek, SN 2011fe, SN 2011iv, SN 2012cg, SN 2013dy, and SN 2014J, respectively.

6 FUTURE WORK

Future work goes here.

REFERENCES

- Aldenius M., Johansson S., Murphy M. T., 2006, MNRAS, 370, 444
 Foley R. J., 2013, MNRAS, 435, 273
 Foley R. J. et al., 2014, ArXiv e-prints
 Foley R. J., Kirshner R. P., 2013a, ApJ, 769, L1
 Foley R. J., Kirshner R. P., 2013b, ApJ, 769, L1
 Foley R. J. et al., 2012, ApJ, 753, L5
 Goobar A. et al., 2014, ApJ, 784, L12
 Graham M. L. et al., 2015, ApJ, 801, 136
 Kirshner R. P. et al., 1993, ApJ, 415, 589
 Leonard D. C., Filippenko A. V., 2001, PASP, 113, 920
 Pan Y.-C. et al., 2015, ArXiv e-prints
 Silverman J. M. et al., 2012, ApJ, 756, L7

Table 2. SNe Properties

SN	Host Galaxy	Host Galaxy Redshift (z)	Host Galaxy Velocity (km s^{-1})	Right Ascension	Declination	Distance Modulus
<i>SN1992A</i>	<i>NGC1380</i>	0.006261	1877	03h36m27.4s	−34d57m31s	31.72
<i>SN2011by</i>	<i>NGC3972</i>	0.002843	852	11h55m45.5s	+55d19m32s	32.01
<i>SN2011ek</i>	<i>NGC918</i>	0.005027	1507	02h25m48.9s	+18d32m00s	32.33
<i>SN2011fe</i>	<i>M101</i>	0.000804	241	14h03m05.8s	+54d16m25s	29.06
<i>SN2011iv</i>	<i>NGC1404</i>	0.006494	1947	03h38m51.3s	−35d35m32s	31.39(<i>Galaxy</i>)
<i>SN2012cg</i>	<i>NGC4424</i>	0.001458	437	12h27m12.8s	+09d25m13s	30.9
<i>SN2013dy</i>	<i>NGC7250</i>	0.003889	1166	22h18m17.6s	+40d34m10s	30.68(<i>Galaxy</i>)
<i>SN2014J</i>	<i>M82</i>	0.000677	203	09h55m42.1s	+69d40m26s	27.57

Table 3. Observing Log

UT (date)	Phase (days)	Instrument	Grating	Exposure Time (sec)	Dataset	PI	Proposal ID
SN 1992A							
1992Jan24	4.98	FOS/RD	MIRROR	40	Y0VQ0101T	KIRSHNER	4016
1992Jan24	4.98	FOS/RD	MIRROR	40	Y0VQ0102T	KIRSHNER	4016
1992Jan24	4.98	FOS/RD	G160L	1499.99	Y0VQ0103T	KIRSHNER	4016
1992Jan24	4.98	FOS/RD	G270H	1499.99	Y0VQ0104T	KIRSHNER	4016
1992Jan24	4.98	FOS/RD	G400H	999.99	Y0VQ0105T	KIRSHNER	4016
1992Jan24	4.98	GHR	MIRROR – N2	0.2	Z0VQ0506T	KIRSHNER	4016
1992Jan24	4.98	GHR	G270M	3916.8	Z0VQ0508T	KIRSHNER	4016
1992Mar04	44.83	FOS/RD	MIRROR	0.49	Y0WA0201T	KIRSHNER	4022
1992Mar04	44.83	FOS/RD	G160L	1349.99	Y0WA0202T	KIRSHNER	4022
1992Mar04	44.83	FOS/RD	G160L	1349.99	Y0WA0203T	KIRSHNER	4022
1992Mar04	44.83	FOS/RD	G270H	1349.99	Y0WA0204T	KIRSHNER	4022
1992Mar04	44.83	FOS/RD	G270H	1349.99	Y0WA0205T	KIRSHNER	4022
1992Mar04	44.83	FOS/RD	G400H	1800	Y0WA0206T	KIRSHNER	4022
1992Nov05	289.58	FOS/RD	MIRROR	145.45	Y1670101T	KIRSHNER	4252
1992Nov05	289.58	FOS/RD	G160L	1999.98	Y1670102T	KIRSHNER	4252
1992Nov05	289.58	FOS/RD	G160L	1999.98	Y1670103T	KIRSHNER	4252
1992Nov05	289.58	FOS/RD	G160L	1999.98	Y1670104T	KIRSHNER	4252
1992Nov05	289.58	FOS/RD	G270H	1999.98	Y1670105T	KIRSHNER	4252
1992Nov05	289.58	FOS/RD	G270H	1999.98	Y1670106T	KIRSHNER	4252
1992Nov05	289.58	FOS/RD	G270H	1999.98	Y1670107T	KIRSHNER	4252
1992Nov05	289.58	FOS/RD	G400H	1999.98	Y1670108T	KIRSHNER	4252
1992Nov05	289.58	FOS/RD	G400H	1999.98	Y1670109T	KIRSHNER	4252
SN 2011by							
2011Apr30	−9.31	STIS/CCD	MIRVIS	4.1	OBND08D2Q	ELLIS	12298
2011Apr30	−9.31	STIS/CCD	G430L	2262.9	OBND08010	ELLIS	12298
2011Apr30	−9.31	STIS/CCD	MIRVIS	4.1	OBND13D9Q	ELLIS	12298
2011Apr30	−9.31	STIS/NUV – MAMA	G230L	8300	OBND13010	ELLIS	12298
2011May09	−0.52	STIS/CCD	MIRVIS	4.1	OBND10CZQ	ELLIS	12298
2011May09	−0.52	STIS/CCD	G430L	2262.9	OBND10010	ELLIS	12298
2011May09	−0.52	STIS/CCD	MIRVIS	4.1	OBND14DEQ	ELLIS	12298
2011May09	−0.52	STIS/NUV – MAMA	G230L	5316	OBND14010	ELLIS	12298
SN 2011ek							
2011Aug12	−3.32	STIS/CCD	MIRVIS	4.1	OBND36A1Q	ELLIS	12298
2011Aug12	−3.32	STIS/CCD	G430L	2100	OBND36010	ELLIS	12298
2011Aug12	−3.32	STIS/CCD	MIRVIS	4.1	OBND41APQ	ELLIS	12298
2011Aug12	−3.32	STIS/NUV – MAMA	G230L	8077	OBND41010	ELLIS	12298
2011Aug19	3.53	STIS/CCD	MIRVIS	4.1	OBND38ZZQ	ELLIS	12298
2011Aug19	3.53	STIS/CCD	G430L	2220	OBND38010	ELLIS	12298
2011Aug19	3.53	STIS/CCD	MIRVIS	4.1	OBND42A6Q	ELLIS	12298
2011Aug19	3.53	STIS/NUV – MAMA	G230L	5198	OBND42010	ELLIS	12298
SN 2011fe							
2011Aug28	−13.11	STIS/CCD	MIRVIS	2.1	OBND43MFQ	ELLIS	12298
2011Aug28	−13.11	STIS/CCD	G430L	1200	OBND43010	ELLIS	12298
2011Aug28	−13.11	STIS/CCD	G750L	1002	OBND43020	ELLIS	12298
2011Aug28	−13.11	STIS/CCD	G750L	50	OBND43030	ELLIS	12298
2011Aug28	−13.11	STIS/CCD	MIRVIS	2.1	OBND48MSQ	ELLIS	12298
2011Aug28	−13.11	STIS/NUV – MAMA	G230L	5400	OBND48010	ELLIS	12298
2011Aug31	−10.04	STIS/CCD	MIRVIS	30.1	OBND44RWQ	ELLIS	12298
2011Aug31	−10.04	STIS/CCD	G430L	578	OBND44010	ELLIS	12298
2011Aug31	−10.04	STIS/CCD	G430L	578	OBND44020	ELLIS	12298
2011Aug31	−10.04	STIS/CCD	G750L	410	OBND44030	ELLIS	12298
2011Aug31	−10.04	STIS/CCD	G750L	410	OBND44040	ELLIS	12298
2011Aug31	−10.04	STIS/CCD	G750L	50	OBND44050	ELLIS	12298
2011Aug31	−10.04	STIS/CCD	MIRVIS	30.1	OBND49SLQ	ELLIS	12298
2011Aug31	−10.04	STIS/NUV – MAMA	G230L	2200	OBND49010	ELLIS	12298
2011Sept03	−6.91	STIS/CCD	MIRVIS	20.1	OBND45SJQ	ELLIS	12298

Table 3 (cont'd)

UT (date)	Phase (days)	Instrument	Grating	Exposure Time (sec)	Dataset	PI	Proposal ID
2011Sept03	−6.91	STIS/CCD	G230LB	1320	OBND45010	ELLIS	12298
2011Sept03	−6.91	STIS/CCD	G430L	195	OBND45020	ELLIS	12298
2011Sept03	−6.91	STIS/CCD	G750L	195	OBND45030	ELLIS	12298
2011Sept03	−6.91	STIS/CCD	G750L	50	OBND45040	ELLIS	12298
2011Sept07	−2.95	STIS/CCD	MIRVIS	20.1	OBND460DQ	ELLIS	12298
2011Sept07	−2.95	STIS/CCD	G230LB	530	OBND46010	ELLIS	12298
2011Sept07	−2.95	STIS/CCD	G230LB	530	OBND46020	ELLIS	12298
2011Sept07	−2.95	STIS/CCD	G430L	80	OBND46030	ELLIS	12298
2011Sept07	−2.95	STIS/CCD	G430L	80	OBND46040	ELLIS	12298
2011Sept07	−2.95	STIS/CCD	G750L	80	OBND46050	ELLIS	12298
2011 Sept 07	−2.95	STIS/CCD	G750L	80	OBND46060	ELLIS	12298
2011Sept07	−2.95	STIS/CCD	G750L	50	OBND46070	ELLIS	12298
2011Sept10	0.04	STIS/CCD	MIRVIS	20.1	OBND47G5Q	ELLIS	12298
2011Sept10	0.04	STIS/CCD	G230LB	530	OBND47010	ELLIS	12298
2011Sept10	0.04	STIS/CCD	G230LB	530	OBND47020	ELLIS	12298
2011Sept10	0.04	STIS/CCD	G430L	80	OBND47030	ELLIS	12298
2011Sept10	0.04	STIS/CCD	G430L	80	OBND47040	ELLIS	12298
2011Sept10	0.04	STIS/CCD	G750L	80	OBND47050	ELLIS	12298
2011Sept10	0.04	STIS/CCD	G750L	80	OBND47060	ELLIS	12298
2011Sept10	0.04	STIS/CCD	G750L	50	OBND47070	ELLIS	12298
2011Sept13	3.25	STIS/CCD	MIRVIS	20.1	OBND50LMQ	ELLIS	12298
2011Sept13	3.25	STIS/CCD	G230LB	415	OBND50010	ELLIS	12298
2011Sept13	3.25	STIS/CCD	G230LB	415	OBND50020	ELLIS	12298
2011Sept13	3.25	STIS/CCD	G430L	80	OBND50030	ELLIS	12298
2011Sept13	3.25	STIS/CCD	G430L	80	OBND50040	ELLIS	12298
2011Sept13	3.25	STIS/CCD	G750L	70	OBND50050	ELLIS	12298
2011Sept13	3.25	STIS/CCD	G750L	70	OBND50060	ELLIS	12298
2011Sept13	3.25	STIS/CCD	G750L	50	OBND50070	ELLIS	12298
2011Sept13	3.25	STIS/FUV – MAMA	G140L	2680	OBND50080	ELLIS	12298
2011Sept13	3.25	STIS/FUV – MAMA	G140L	2930	OBND50090	ELLIS	12298
2011Sept13	3.25	STIS/FUV – MAMA	G140L	2930	OBND500A0	ELLIS	12298
2011Sept19	9.15	STIS/CCD	MIRVIS	30.1	OBND51DRQ	ELLIS	12298
2011Sept19	9.15	STIS/CCD	G230LB	500	OBND51010	ELLIS	12298
2011Sept19	9.15	STIS/CCD	G230LB	500	OBND51020	ELLIS	12298
2011Sept19	9.15	STIS/CCD	G430L	80	OBND51030	ELLIS	12298
2011Sept19	9.15	STIS/CCD	G430L	80	OBND51040	ELLIS	12298
2011Sept19	9.15	STIS/CCD	G750L	70	OBND51050	ELLIS	12298
2011Sept19	9.15	STIS/CCD	G750L	70	OBND51060	ELLIS	12298
2011Sept19	9.15	STIS/CCD	G750L	50	OBND51070	ELLIS	12298
2011Sept19	9.15	STIS/NUV – MAMA	G230L	2720	OBND51080	ELLIS	12298
2011Oct01	20.69	STIS/CCD	MIRVIS	40.1	OBND52S6Q	ELLIS	12298
2011Oct01	20.69	STIS/CCD	G430L	600	OBND52010	ELLIS	12298
2011Oct01	20.69	STIS/CCD	G430L	600	OBND52020	ELLIS	12298
2011Oct01	20.69	STIS/CCD	G750L	190	OBND52030	ELLIS	12298
2011Oct01	20.69	STIS/CCD	G750L	190	OBND52040	ELLIS	12298
2011Oct01	20.69	STIS/CCD	G750L	50	OBND52050	ELLIS	12298
2011Oct01	20.69	STIS/NUV – MAMA	G230L	1350	OBND52060	ELLIS	12298
2011Oct01	20.69	STIS/NUV – MAMA	G230L	1350	OBND52070	ELLIS	12298
2011Oct07	26.69	STIS/CCD	MIRVIS	0.9	OBND53X3Q	ELLIS	12298
2011Oct07	26.69	STIS/CCD	G430L	660	OBND53010	ELLIS	12298
2011Oct07	26.69	STIS/CCD	G430L	660	OBND53020	ELLIS	12298
2011Oct07	26.69	STIS/CCD	G750L	310	OBND53030	ELLIS	12298
2011Oct07	26.69	STIS/CCD	G750L	310	OBND53040	ELLIS	12298
2011Oct07	26.69	STIS/CCD	G750L	50	OBND53050	ELLIS	12298
2011Oct07	26.69	STIS/NUV – MAMA	G230L	1500	OBND53060	ELLIS	12298
2011Oct07	26.69	STIS/NUV – MAMA	G230L	1500	OBND53070	ELLIS	12298
2011Oct21	40.45	STIS/CCD	MIRVIS	1.1	OBND54AVQ	ELLIS	12298

Table 3 (cont'd)

UT (date)	Phase (days)	Instrument	Grating	Exposure Time (sec)	Dataset	PI	Proposal ID
2011Oct21	40.45	STIS/CCD	G430L	610	OBND54010	ELLIS	12298
2011Oct21	40.45	STIS/CCD	G430L	610	OBND54020	ELLIS	12298
2011Oct21	40.45	STIS/CCD	G750L	420	OBND54030	ELLIS	12298
2011Oct21	40.45	STIS/CCD	G750L	420	OBND54040	ELLIS	12298
2011Oct21	40.45	STIS/CCD	G750L	50	OBND54050	ELLIS	12298
2011Oct21	40.45	STIS/NUV – MAMA	G230L	1500	OBND54060	ELLIS	12298
2011Oct21	40.45	STIS/NUV – MAMA	G230L	1500	OBND54070	ELLIS	12298
SN 2011iv							
2011Dec11	0.6	STIS/CCD	MIRVIS	0.3	OBWR11SWQ	FOLEY	12592
2011Dec11	0.6	STIS/NUV – MAMA	G230L	2200	OBWR11010	FOLEY	12592
2011Dec11	0.6	STIS/NUV – MAMA	G230L	1350	OBWR11020	FOLEY	12592
2011Dec11	0.6	STIS/CCD	G430L	100	OBWR11030	FOLEY	12592
2011Dec11	0.6	STIS/CCD	G430L	100	OBWR11040	FOLEY	12592
2011Dec11	0.6	STIS/CCD	G750L	100	OBWR11050	FOLEY	12592
2011Dec11	0.6	STIS/CCD	G750L	100	OBWR11060	FOLEY	12592
2011Dec11	0.6	STIS/CCD	G750L	50	OBWR11070	FOLEY	12592
2011Dec15	5.41	STIS/CCD	MIRVIS0.3	OBWR12B1Q	FOLEY	12592	
2011Dec15	5.41	STIS/NUV – MAMA	G230L	1400	OBWR12010	FOLEY	12592
2011Dec15	5.41	STIS/CCD	G430L	100	OBWR12020	FOLEY	12592
2011Dec15	5.41	STIS/CCD	G750L	100	OBWR12030	FOLEY	12592
2011Dec15	5.41	STIS/CCD	G750L	50	OBWR12040	FOLEY	12592
2011Dec20	10.15	STIS/CCD	MIRVIS	0.3	OBWR13MBQ	FOLEY	12592
2011Dec20	10.15	STIS/NUV – MAMA	G230L	1400	OBWR13010	FOLEY	12592
2011Dec20	10.15	STIS/CCD	G430L	100	OBWR13020	FOLEY	12592
2011Dec20	10.15	STIS/CCD	G750L	100	OBWR13030	FOLEY	12592
2011Dec20	10.15	STIS/CCD	G750L	50	OBWR13040	FOLEY	12592
2011Dec24	13.99	STIS/CCD	MIRVIS	0.3	OBWR14NFQ	FOLEY	12592
2011Dec24	13.99	STIS/NUV – MAMA	G230L	1400	OBWR14010	FOLEY	12592
2011Dec24	13.99	STIS/CCD	G430L	100	OBWR14020	FOLEY	12592
2011Dec24	13.99	STIS/CCD	G750L	100	OBWR14030	FOLEY	12592
2011Dec24	13.99	STIS/CCD	G750L	50	OBWR14040	FOLEY	12592
2011Dec28	17.82	STIS/CCD	MIRVIS	0.3	OBWR15Q0Q	FOLEY	12592
2011Dec28	17.82	STIS/NUV – MAMA	G230L	1400	OBWR15010	FOLEY	12592
2011Dec28	17.82	STIS/CCD	G430L	100	OBWR15020	FOLEY	12592
2011Dec28	17.82	STIS/CCD	G750L	100	OBWR15030	FOLEY	12592
2011Dec28	17.82	STIS/CCD	G750L	50	OBWR15040	FOLEY	12592
2012Jan01	21.72	STIS/CCD	MIRVIS	0.3	OBWR16ODQ	FOLEY	12592
2012Jan01	21.72	STIS/NUV – MAMA	G230L	1400	OBWR16010	FOLEY	12592
2012Jan01	21.72	STIS/CCD	G430L	100	OBWR16020	FOLEY	12592
2012Jan01	21.72	STIS/CCD	G750L	100	OBWR16030	FOLEY	12592
2012Jan01	21.72	STIS/CCD	G750L	50	OBWR16040	FOLEY	12592
2012Jan09	29.52	STIS/CCD	MIRVIS	0.3	OBWR17AIQ	FOLEY	12592
2012Jan09	29.52	STIS/NUV – MAMA	G230L	1400	OBWR17010	FOLEY	12592
2012Jan09	29.52	STIS/CCD	G430L	100	OBWR17020	FOLEY	12592
2012Jan09	29.52	STIS/CCD	G750L	100	OBWR17030	FOLEY	12592
2012Jan09	29.52	STIS/CCD	G750L	50	OBWR17040	FOLEY	12592
SN 2012cg							
2012June04	2.5	STIS/CCD	MIRVIS	0.5	OBXB92E9Q	GOOBAR	12582
2012June04	2.5	STIS/CCD	G230LB	856	OBXB92010	GOOBAR	12582
2012June04	2.5	STIS/CCD	G230LB	856	OBXB92020	GOOBAR	12582
2012June04	2.5	STIS/CCD	G430L	156	OBXB92030	GOOBAR	12582
2012June04	2.5	STIS/CCD	G430L	156	OBXB92040	GOOBAR	12582
2012June18	16.37	STIS/CCD	MIRVIS	0.5	OBXB93ELQ	GOOBAR	12582
2012June18	16.37	STIS/CCD	G230LB	856	OBXB93010	GOOBAR	12582
2012June18	16.37	STIS/CCD	G230LB	856	OBXB93020	GOOBAR	12582
2012June18	16.37	STIS/CCD	G430L	156	OBXB93030	GOOBAR	12582
2012June18	16.37	STIS/CCD	G430L	156	OBXB93040	GOOBAR	12582

Table 3 (cont'd)

UT (date)	Phase (days)	Instrument	Grating	Exposure Time (sec)	Dataset	PI	Proposal ID
SN 2013dy							
2013July21	−6.17	<i>STIS/CCD</i>	<i>MIRVIS</i>	0.3	<i>OCB101HWQ</i>	<i>FOLEY</i>	13286
2013July21	−6.17	<i>STIS/NUV – MAMA</i>	<i>G230L</i>	2200	<i>OCB101010</i>	<i>FOLEY</i>	13286
2013July21	−6.17	<i>STIS/NUV – MAMA</i>	<i>G230L</i>	1418	<i>OCB101020</i>	<i>FOLEY</i>	13286
2013July21	−6.17	<i>STIS/CCD</i>	<i>G430L</i>	336	<i>OCB101030</i>	<i>FOLEY</i>	13286
2013July21	−6.17	<i>STIS/CCD</i>	<i>G750L</i>	336	<i>OCB101040</i>	<i>FOLEY</i>	13286
2013July21	−6.17	<i>STIS/CCD</i>	<i>G750L</i>	50	<i>OCB101050</i>	<i>FOLEY</i>	13286
2013July25	−2.09	<i>STIS/CCD</i>	<i>MIRVIS</i>	0.3	<i>OCB102F7Q</i>	<i>FOLEY</i>	13286
2013July25	−2.09	<i>STIS/NUV – MAMA</i>	<i>G230L</i>	1382	<i>OCB102010</i>	<i>FOLEY</i>	13286
2013July25	−2.09	<i>STIS/CCD</i>	<i>G430L</i>	64	<i>OCB102020</i>	<i>FOLEY</i>	13286
2013July25	−2.09	<i>STIS/CCD</i>	<i>G750L</i>	64	<i>OCB102030</i>	<i>FOLEY</i>	13286
2013July25	−2.09	<i>STIS/CCD</i>	<i>G750L</i>	50	<i>OCB102040</i>	<i>FOLEY</i>	13286
2013July27	−0.37	<i>STIS/CCD</i>	<i>MIRVIS</i>	0.3	<i>OCB103OJQ</i>	<i>FOLEY</i>	13286
2013July27	−0.37	<i>STIS/NUV – MAMA</i>	<i>G230L</i>	1382	<i>OCB103010</i>	<i>FOLEY</i>	13286
2013July27	−0.37	<i>STIS/CCD</i>	<i>G430L</i>	64	<i>OCB103020</i>	<i>FOLEY</i>	13286
2013July27	−0.37	<i>STIS/CCD</i>	<i>G750L</i>	64	<i>OCB103030</i>	<i>FOLEY</i>	13286
2013July27	−0.37	<i>STIS/CCD</i>	<i>G750L</i>	50	<i>OCB103040</i>	<i>FOLEY</i>	13286
2013July29	1.61	<i>STIS/CCD</i>	<i>MIRVIS</i>	0.3	<i>OCB104B1Q</i>	<i>FOLEY</i>	13286
2013July29	1.61	<i>STIS/NUV – MAMA</i>	<i>G230L</i>	1382	<i>OCB104010</i>	<i>FOLEY</i>	13286
2013July29	1.61	<i>STIS/CCD</i>	<i>G430L</i>	64	<i>OCB104020</i>	<i>FOLEY</i>	13286
2013July29	1.61	<i>STIS/CCD</i>	<i>G750L</i>	64	<i>OCB104030</i>	<i>FOLEY</i>	13286
2013July29	1.61	<i>STIS/CCD</i>	<i>G750L</i>	50	<i>OCB104040</i>	<i>FOLEY</i>	13286
2013Aug01	4.85	<i>STIS/CCD</i>	<i>MIRVIS</i>	0.3	<i>OCB105Z2Q</i>	<i>FOLEY</i>	13286
2013Aug01	4.85	<i>STIS/NUV – MAMA</i>	<i>G230L</i>	1382	<i>OCB105010</i>	<i>FOLEY</i>	13286
2013Aug01	4.85	<i>STIS/CCD</i>	<i>G430L</i>	64	<i>OCB105020</i>	<i>FOLEY</i>	13286
2013Aug01	4.85	<i>STIS/CCD</i>	<i>G750L</i>	64	<i>OCB105030</i>	<i>FOLEY</i>	13286
2013Aug01	4.85	<i>STIS/CCD</i>	<i>G750L</i>	50	<i>OCB105040</i>	<i>FOLEY</i>	13286
2013Aug05	8.76	<i>STIS/CCD</i>	<i>MIRVIS</i>	0.3	<i>OCB106BUQ</i>	<i>FOLEY</i>	13286
2013Aug05	8.76	<i>STIS/NUV – MAMA</i>	<i>G230L</i>	1382	<i>OCB106010</i>	<i>FOLEY</i>	13286
2013Aug05	8.76	<i>STIS/CCD</i>	<i>G430L</i>	64	<i>OCB106020</i>	<i>FOLEY</i>	13286
2013Aug05	8.76	<i>STIS/CCD</i>	<i>G750L</i>	64	<i>OCB106030</i>	<i>FOLEY</i>	13286
2013Aug05	8.76	<i>STIS/CCD</i>	<i>G750L</i>	50	<i>OCB106040</i>	<i>FOLEY</i>	13286
2013Aug09	12.36	<i>STIS/CCD</i>	<i>MIRVIS</i>	0.3	<i>OCB107ZGQ</i>	<i>FOLEY</i>	13286
2013Aug09	12.36	<i>STIS/NUV – MAMA</i>	<i>G230L</i>	1382	<i>OCB107010</i>	<i>FOLEY</i>	13286
2013Aug09	12.36	<i>STIS/CCD</i>	<i>G430L</i>	64	<i>OCB107020</i>	<i>FOLEY</i>	13286
2013Aug09	12.36	<i>STIS/CCD</i>	<i>G750L</i>	64	<i>OCB107030</i>	<i>FOLEY</i>	13286
2013Aug09	12.36	<i>STIS/CCD</i>	<i>G750L</i>	50	<i>OCB107040</i>	<i>FOLEY</i>	13286
2013Aug11	14.38	<i>STIS/CCD</i>	<i>MIRVIS</i>	0.3	<i>OCB108NEQ</i>	<i>FOLEY</i>	13286
2013Aug11	14.38	<i>STIS/NUV – MAMA</i>	<i>G230L</i>	1382	<i>OCB108010</i>	<i>FOLEY</i>	13286
2013Aug11	14.38	<i>STIS/CCD</i>	<i>G430L</i>	64	<i>OCB108020</i>	<i>FOLEY</i>	13286
2013Aug11	14.38	<i>STIS/CCD</i>	<i>G750L</i>	64	<i>OCB108030</i>	<i>FOLEY</i>	13286
2013Aug11	14.38	<i>STIS/CCD</i>	<i>G750L</i>	50	<i>OCB108040</i>	<i>FOLEY</i>	13286
2013Aug15	18.22	<i>STIS/CCD</i>	<i>MIRVIS</i>	0.3	<i>OCB109R2Q</i>	<i>FOLEY</i>	13286
2013Aug15	18.22	<i>STIS/NUV – MAMA</i>	<i>G230L</i>	1382	<i>OCB109010</i>	<i>FOLEY</i>	13286
2013Aug15	18.22	<i>STIS/CCD</i>	<i>G430L</i>	64	<i>OCB109020</i>	<i>FOLEY</i>	13286
2013Aug15	18.22	<i>STIS/CCD</i>	<i>G750L</i>	64	<i>OCB109030</i>	<i>FOLEY</i>	13286
2013Aug15	18.22	<i>STIS/CCD</i>	<i>G750L</i>	50	<i>OCB109040</i>	<i>FOLEY</i>	13286
2013Aug17	21.17	<i>STIS/CCD</i>	<i>MIRVIS</i>	0.3	<i>OCB110EBQ</i>	<i>FOLEY</i>	13286
2013Aug17	21.17	<i>STIS/NUV – MAMA</i>	<i>G230L</i>	2200	<i>OCB110010</i>	<i>FOLEY</i>	13286
2013Aug17	21.17	<i>STIS/NUV – MAMA</i>	<i>G230L</i>	1418	<i>OCB110020</i>	<i>FOLEY</i>	13286
2013Aug17	21.17	<i>STIS/CCD</i>	<i>G430L</i>	336	<i>OCB110030</i>	<i>FOLEY</i>	13286
2013Aug17	21.17	<i>STIS/CCD</i>	<i>G750L</i>	336	<i>OCB110040</i>	<i>FOLEY</i>	13286
2013Aug17	21.17	<i>STIS/CCD</i>	<i>G750L</i>	50	<i>OCB110050</i>	<i>FOLEY</i>	13286
SN 2014J							
2014Jan26	−6.5	<i>STIS/CCD</i>	<i>MIRVIS</i>	0.3	<i>OCB150EZQ</i>	<i>FOLEY</i>	13286
2014Jan26	−6.5	<i>STIS/NUV – MAMA</i>	<i>G230L</i>	2235	<i>OCB150010</i>	<i>FOLEY</i>	13286
2014Jan26	−6.5	<i>STIS/NUV – MAMA</i>	<i>G230L</i>	2807	<i>OCB150020</i>	<i>FOLEY</i>	13286

Table 3 (cont'd)

UT (date)	Phase (days)	Instrument	Grating	Exposure Time (sec)	Dataset	PI	Proposal ID
2014Jan26	-6.5	STIS/NUV – MAMA	G230L	2807	OCB150030	FOLEY	13286
2014Jan26	-6.5	STIS/NUV – MAMA	G230L	1724	OCB150040	FOLEY	13286
2014Jan26	-6.5	STIS/CCD	G430L	300	OCB150050	FOLEY	13286
2014Jan26	-6.5	STIS/CCD	G750L	200	OCB150060	FOLEY	13286
2014Jan26	-6.5	STIS/CCD	G750L	50	OCB150070	FOLEY	13286
2014Jan28	-4.5	STIS/CCD	MIRVIS	0.3	OCB151JRQ	FOLEY	13286
2014Jan28	-4.5	STIS/NUV – MAMA	G230L	2255	OCB151010	FOLEY	13286
2014Jan28	-4.5	STIS/NUV – MAMA	G230L	1747	OCB151020	FOLEY	13286
2014Jan28	-4.5	STIS/CCD	G430L	160	OCB151030	FOLEY	13286
2014Jan28	-4.5	STIS/CCD	G750L	100	OCB151040	FOLEY	13286
2014Jan28	-4.5	STIS/CCD	G750L	50	OCB151050	FOLEY	13286
2014Jan30	-2.5	STIS/CCD	MIRVIS	0.3	OCB152SXQ	FOLEY	13286
2014Jan30	-2.5	STIS/NUV – MAMA	G230L	2255	OCB152010	FOLEY	13286
2014Jan30	-2.5	STIS/NUV – MAMA	G230L	1747	OCB152020	FOLEY	13286
2014Jan30	-2.5	STIS/CCD	G430L	160	OCB152030	FOLEY	13286
2014Jan30	-2.5	STIS/CCD	G750L	100	OCB152040	FOLEY	13286
2014Jan30	-2.5	STIS/CCD	G750L	50	OCB152050	FOLEY	13286
2014Feb01	-0.5	STIS/CCD	MIRVIS	0.3	OCB153CVQ	FOLEY	13286
2014Feb01	-0.5	STIS/NUV – MAMA	G230L	2255	OCB153010	FOLEY	13286
2014Feb01	-0.5	STIS/NUV – MAMA	G230L	1747	OCB153020	FOLEY	13286
2014Feb01	-0.5	STIS/CCD	G430L	160	OCB153030	FOLEY	13286
2014Feb01	-0.5	STIS/CCD	G750L	100	OCB153040	FOLEY	13286
2014Feb01	-0.5	STIS/CCD	G750L	50	OCB153050	FOLEY	13286
2014Feb04	2.5	STIS/CCD	MIRVIS	0.3	OCB154M5Q	FOLEY	13286
2014Feb04	2.5	STIS/NUV – MAMA	G230L	2255	OCB154010	FOLEY	13286
2014Feb04	2.5	STIS/NUV – MAMA	G230L	153.66	OCB154020	FOLEY	13286
2014Feb04	2.5	STIS/CCD	G430L	160	OCB154030	FOLEY	13286
2014Feb04	2.5	STIS/CCD	G750L	100	OCB154040	FOLEY	13286
2014Feb04	2.5	STIS/CCD	G750L	50	OCB154050	FOLEY	13286
2014Feb08	6.5	STIS/CCD	MIRVIS	0.3	OCB155IRQ	FOLEY	13286
2014Feb08	6.5	STIS/NUV – MAMA	G230L	2255	OCB155010	FOLEY	13286
2014Feb08	6.5	STIS/NUV – MAMA	G230L	1747	OCB155020	FOLEY	13286
2014Feb08	6.5	STIS/CCD	G430L	160	OCB155030	FOLEY	13286
2014Feb08	6.5	STIS/CCD	G750L	100	OCB155040	FOLEY	13286
2014Feb08	6.5	STIS/CCD	G750L	50	OCB155050	FOLEY	13286
2014Feb10	8.49	STIS/CCD	MIRVIS	0.3	OCB156DBQ	FOLEY	13286
2014Feb10	8.49	STIS/NUV – MAMA	G230L	2255	OCB156010	FOLEY	13286
2014Feb10	8.49	STIS/NUV – MAMA	G230L	1747	OCB156020	FOLEY	13286
2014Feb10	8.49	STIS/CCD	G430L	160	OCB156030	FOLEY	13286
2014Feb10	8.49	STIS/CCD	G750L	100	OCB156040	FOLEY	13286
2014Feb10	8.49	STIS/CCD	G750L	50	OCB156050	FOLEY	13286
2014Feb13	11.49	STIS/CCD	MIRVIS	0.3	OCB157S6Q	FOLEY	13286
2014Feb13	11.49	STIS/NUV – MAMA	G230L	2255	OCB157010	FOLEY	13286
2014Feb13	11.49	STIS/NUV – MAMA	G230L	1747	OCB157020	FOLEY	13286
2014Feb13	11.49	STIS/CCD	G430L	160	OCB157030	FOLEY	13286
2014Feb13	11.49	STIS/CCD	G750L	100	OCB157040	FOLEY	13286
2014Feb13	11.49	STIS/CCD	G750L	50	OCB157050	FOLEY	13286
2014Feb16	14.49	STIS/CCD	MIRVIS	0.3	OCB158S9Q	FOLEY	13286
2014Feb16	14.49	STIS/NUV – MAMA	G230L	2255	OCB158010	FOLEY	13286
2014Feb16	14.49	STIS/NUV – MAMA	G230L	1747	OCB158020	FOLEY	13286
2014Feb16	14.49	STIS/CCD	G430L	160	OCB158030	FOLEY	13286
2014Feb16	14.49	STIS/CCD	G750L	100	OCB158040	FOLEY	13286
2014Feb16	14.49	STIS/CCD	G750L	50	OCB158050	FOLEY	13286
2014Feb26	24.05	STIS/CCD	MIRVIS	0.3	OCB159IAQ	FOLEY	13286
2014Feb26	24.05	STIS/NUV – MAMA	G230L	2235	OCB159010	FOLEY	13286
2014Feb26	24.05	STIS/NUV – MAMA	G230L	2807	OCB159020	FOLEY	13286
2014Feb26	24.05	STIS/NUV – MAMA	G230L	2807	OCB159030	FOLEY	13286

Table 3 (cont'd)

UT (date)	Phase (days)	Instrument	Grating	Exposure Time (sec)	Dataset	PI	Proposal ID
2014Feb26	24.05	<i>STIS/NUV – MAMA</i>	<i>G230L</i>	1724	<i>OCB159040</i>	<i>FOLEY</i>	13286
2014Feb26	24.05	<i>STIS/CCD</i>	<i>G430L</i>	300	<i>OCB159050</i>	<i>FOLEY</i>	13286
2014Feb26	24.05	<i>STIS/CCD</i>	<i>G750L</i>	200	<i>OCB159060</i>	<i>FOLEY</i>	13286
2014Feb26	24.05	<i>STIS/CCD</i>	<i>G750L</i>	50	<i>OCB159070</i>	<i>FOLEY</i>	13286
2014Feb26	24.05	<i>STIS/CCD</i>	<i>MIRVIS</i>	0.3	<i>OCB160JZQ</i>	<i>FOLEY</i>	13286
2014Feb26	24.05	<i>STIS/NUV – MAMA</i>	<i>G230L</i>	2255	<i>OCB160010</i>	<i>FOLEY</i>	13286

Table 4. Measurements of Observed SNe

UT (days)	Phase (d)	FeII (2344.22 Å)	FeII (2374.46 Å)	FeII (2382.76 Å)	FeII (2586.65 Å)	FeII (2600.17 Å)	MgII (2796.35 Å)	MgII (2803.53 Å)	MgI (2852.96 Å)
19920124.21	4.98	0.51	1.09	1.26	SN 1992A	1.51	0.52	0.25	0.55
19920304.31	44.83	1.74	0.97	1.35		2.62	1.18	1.15	2.92
19921105.59	289.58	6.16	33.14	27.6		5.47	2.71	2.4	2.25
20110430.56	-9.31	0.0	0.0	0.0	SN 2011by	0.0	1.39 ^{+0.01} _{-0.02}	1.37 ^{+0.01} _{-0.02}	0.74 ^{+0.28} _{-0.26}
20110509.38	-0.52	0.47 ^{+0.01} _{-0.01}	0.86 ^{+1.35} _{-0.43}	0.4 ^{+0.66} _{-0.02}		1.25 ^{+0.65} _{-0.67}	2.21 ^{+0.07} _{-0.06}	2.83 ^{+0.1} _{-0.08}	0.61 ^{+0.26} _{-0.26}
20110812.56	-3.32	10.1	17.25	21.41		4.28	1.97	2.01	0.76
20110819.45	3.53	41.69	6.19	4.93	SN 2011fe	22.72	1.77	2.5	1.29
20110828.17	-13.11	1.52 ^{+0.39} _{-0.01}	0.13 ^{+0.02} _{-0.04}	1.41 ^{+0.72} _{-0.22}		1.08 ^{+0.03} _{-0.03}	2.72 ^{+0.09} _{-0.1}	2.59 ^{+0.07} _{-0.07}	0.39 ^{+0.03} _{-0.03}
20110831.27	-10.04	1.24 ^{+0.01} _{-0.01}	1.68 ^{+0.11} _{-0.11}	2.11 ^{+0.22} _{-0.22}		1.16 ^{+0.03} _{-0.03}	2.72 ^{+0.1} _{-0.1}	1.99 ^{+0.31} _{-0.31}	0.37 ^{+0.11} _{-0.11}
20110903.43	-6.91	1.28 ^{+0.02} _{-0.02}	0.96 ^{+0.16} _{-0.16}	1.92 ^{+0.26} _{-0.26}	SN 2011iv	1.80 ^{+0.01} _{-0.01}	2.94 ^{+0.28} _{-0.28}	2.61 ^{+0.4} _{-0.4}	0.68 ^{+0.12} _{-0.12}
20110907.42	-2.95	1.48 ^{+0.03} _{-0.03}	0.73 ^{+0.02} _{-0.02}	1.85 ^{+0.26} _{-0.26}		1.79 ^{+0.15} _{-0.15}	3.0 ^{+0.26} _{-0.26}	2.74 ^{+0.45} _{-0.45}	0.61 ^{+0.17} _{-0.17}
20110910.44	0.04	1.24 ^{+0.13} _{-0.13}	0.73 ^{+0.1} _{-0.1}	1.68 ^{+0.02} _{-0.02}		1.56 ^{+0.01} _{-0.01}	2.86 ^{+0.17} _{-0.17}	2.64 ^{+0.03} _{-0.03}	0.67 ^{+0.15} _{-0.15}
20110913.68	3.25	1.85 ^{+0.07} _{-0.07}	1.3 ^{+0.23} _{-0.23}	2.0 ^{+0.22} _{-0.22}	SN 2012eg	1.31 ^{+0.12} _{-0.12}	2.9 ^{+0.06} _{-0.06}	2.11 ^{+0.28} _{-0.28}	0.39 ^{+0.01} _{-0.01}
20110919.63	9.15	1.25 ^{+0.02} _{-0.02}	0.68 ^{+0.02} _{-0.02}	1.72 ^{+0.01} _{-0.01}		1.53 ^{+0.14} _{-0.14}	2.76 ^{+0.08} _{-0.08}	2.56 ^{+0.18} _{-0.18}	0.48 ^{+0.0} _{-0.0}
20111001.27	20.69	1.49 ^{+0.07} _{-0.07}	0.89 ^{+0.02} _{-0.02}	2.03 ^{+0.24} _{-0.24}		1.27 ^{+0.23} _{-0.23}	2.61 ^{+0.23} _{-0.23}	2.19 ^{+0.01} _{-0.01}	0.54 ^{+0.0} _{-0.0}
20111007.32	26.69	2.15 ^{+0.07} _{-0.07}	0.54 ^{+0.2} _{-0.2}	1.26 ^{+0.1} _{-0.1}	SN 2012dy	1.24 ^{+0.01} _{-0.01}	2.27 ^{+0.04} _{-0.04}	2.62 ^{+0.37} _{-0.37}	0.77 ^{+0.01} _{-0.01}
20111021.2	40.45	0.74 ^{+0.3} _{-0.3}	0.43 ^{+0.17} _{-0.17}	1.26 ^{+0.2} _{-0.2}		2.22 ^{+0.5} _{-0.5}	2.54 ^{+0.02} _{-0.02}	2.45 ^{+0.12} _{-0.12}	0.84 ^{+0.02} _{-0.02}
20111211.1	0.6	0.09	0.3	0.06		0.14	0.24	0.07	0.05
20111215.94	5.41	0.26	0.36	0.38	SN 2013dg	0.21	0.25	0.07	0.2
20111220.72	10.15	0.37	0.47	0.33		0.26	0.41	0.26	0.31
20111224.58	13.99	0.49	0.39	0.72		0.45	0.34	0.3	0.18
20111228.44	17.82	0.77	1.16	1.13	SN 2012cg	0.49	0.67	0.35	0.32
20120101.36	21.72	1.07	0.88	1.02		0.61	0.74	0.41	0.73
20120109.21	29.52	1.22	0.83	0.67		0.88	0.82	0.81	0.62
20120604.5	2.5	1.18	0.76	1.13	SN 2013dy	0.36	1.32 ^{+0.01} _{-0.02}	1.32 ^{+0.01} _{-0.02}	0.91 ^{+0.28} _{-0.28}
20120618.4	16.37	2.45	1.42	1.09		1.12	1.93 ^{+0.01} _{-0.01}	1.92 ^{+0.01} _{-0.01}	1.31 ^{+0.28} _{-0.28}
20130721.5	-6.17	2.59 ^{+1.02} _{-1.02}	2.26 ^{+1.15} _{-0.06}	2.25 ^{+1.62} _{-0.05}		1.94 ^{+0.83} _{-0.04}	1.51 ^{+0.0} _{-0.0}	1.51 ^{+0.0} _{-0.0}	0.93 ^{+0.13} _{-0.13}
20130725.61	-2.09	2.28 ^{+0.93} _{-0.93}	0.62	0.65	SN 2013dy	1.31 ^{+0.23} _{-0.23}	1.19 ^{+0.07} _{-0.07}	1.08 ^{+0.05} _{-0.05}	0.76 ^{+0.08} _{-0.08}
20130727.34	-0.37	0.87 ^{+0.02} _{-0.02}	1.22 ^{+0.04} _{-0.04}	1.22 ^{+0.04} _{-0.04}		0.86 ^{+0.06} _{-0.06}	1.23 ^{+0.05} _{-0.05}	1.17 ^{+0.05} _{-0.05}	0.56 ^{+0.23} _{-0.23}
20130729.32	1.61	0.89 ^{+0.11} _{-0.11}	1.26 ^{+0.11} _{-0.11}	1.26 ^{+0.11} _{-0.11}		0.89 ^{+0.16} _{-0.16}	1.37 ^{+0.24} _{-0.24}	1.37 ^{+0.24} _{-0.24}	0.4 ^{+0.23} _{-0.23}
20130801.59	4.85	0.0	0.0	0.0	SN 2013dy	1.13 ^{+0.04} _{-0.04}	1.45 ^{+0.02} _{-0.02}	1.45 ^{+0.02} _{-0.02}	0.71 ^{+0.09} _{-0.09}
20130805.51	8.76	1.03 ^{+0.74} _{-0.74}	1.35 ^{+0.42} _{-0.36}	1.34 ^{+0.39} _{-0.36}		1.63 ^{+0.09} _{-0.09}	1.45 ^{+0.03} _{-0.03}	1.41 ^{+0.26} _{-0.26}	0.6 ^{+0.23} _{-0.23}
20130809.11	12.36	2.78 ^{+0.87} _{-0.87}	2.98 ^{+0.13} _{-0.13}	3.79 ^{+1.6} _{-1.6}		1.16 ^{+0.89} _{-0.89}	1.24 ^{+0.18} _{-0.18}	1.24 ^{+0.18} _{-0.18}	1.12 ^{+0.51} _{-0.51}
20130811.15	14.38	0.0	0.0	0.0	SN 2013dy	2.81 ^{+0.29} _{-0.29}	2.51 ^{+0.03} _{-0.03}	1.9 ^{+0.03} _{-0.03}	0.6 ^{+0.12} _{-0.12}

Table 4 (cont'd)

UT (days)	Phase (d)	Fe II (2344.22 Å)	Fe II (2374.46 Å)	Fe II (2382.76 Å)	Fe II (2586.65 Å)	Fe II (2600.17 Å)	Mg II (2796.35 Å)	Mg II (2803.53 Å)	Mg I (2852.96 Å)
20130815.01	18.22	3.43	1.11	1.11	$0.68^{+0.37}_{-0.31}$	$0.52^{+0.28}_{-0.23}$	$2.76^{+0.53}_{-0.64}$	$1.9^{+0.63}_{-0.73}$	0.5
20130817.94	21.17	0.0	$1.2^{+4.59}_{-0.07}$	$0.72^{+4.6}_{-0.06}$	$0.88^{+0.37}_{-0.32}$ SN 2014J	$0.88^{+0.9}_{-0.02}$	$2.19^{+0.71}_{-0.19}$	$2.19^{+0.55}_{-0.19}$	$0.85^{+0.17}_{-0.17}$
20140126.6	-6.5	22.91	71.66	8.98	2.95	4.78	$2.91^{+0.11}_{-0.11}$	$3.08^{+0.36}_{-0.36}$	$1.76^{+0.21}_{-0.21}$
20140128.44	-4.5	14.58	10.42	17.73	3.61	2.71	$1.93^{+0.37}_{-0.36}$	$1.79^{+0.19}_{-0.2}$	$1.86^{+0.32}_{-0.32}$
20140130.49	-2.5	25.6	70.23	33.27	18.53	5.69	$3.44^{+0.72}_{-0.73}$	$2.63^{+0.77}_{-0.77}$	$1.91^{+0.07}_{-0.08}$
20140201.61	-0.5	36.94	5.79	16.11	4.5	4.5	$4.14^{+0.23}_{-0.23}$	$4.16^{+0.2}_{-0.2}$	$1.27^{+0.5}_{-0.5}$
20140204.73	2.5	13.69	18.55	27.71	26.99	6.6	$2.59^{+1.11}_{-1.11}$	$2.71^{+0.09}_{-0.09}$	$1.99^{+0.95}_{-0.95}$
20140208.53	6.5	32.54	17.55	19.11	6.31	4.21	$4.34^{+0.16}_{-0.16}$	$2.73^{+0.18}_{-0.18}$	$1.61^{+0.08}_{-0.08}$
20140210.44	8.49	22.71	6.14	8.1	9.39	4.09	$2.95^{+0.1}_{-0.1}$	$2.72^{+0.15}_{-0.15}$	$0.96^{+0.07}_{-0.07}$
20140213.29	11.49	93.92	73.85	21.53	16.75	60.77	$3.34^{+0.64}_{-0.63}$	$2.64^{+0.32}_{-0.34}$	$2.87^{+0.74}_{-0.75}$
20140216.41	14.49	15.36	12.76	13.15	12.21	16.73	$2.77^{+0.57}_{-0.58}$	$2.81^{+0.22}_{-0.25}$	$1.2^{+0.21}_{-0.25}$
20140226.07	24.05	15.99	67.91	69.71	19.14	10.51	$5.74^{+0.59}_{-0.59}$	$5.79^{+0.96}_{-0.96}$	$3.46^{+0.26}_{-0.26}$